Seismic Behavior of NPP Structures Subjected to Realistic 3D, Inclined Seismic Motions, in Variable Layered Soil/Rock, on Surface or Embedded Foundations

B. Jeremić[1,2], N. Tafazzoli[1], T. Ancheta[3], N. Orbović[4], A. Blahoianu[4]

[1] University of California, Davis, California, U.S.A.

[2] Lawrence Berkeley National Laboratory, Berkeley, California, U.S.A.

[3] Risk Management Solutions, Inc., Newark, California, U.S.A.

[4] Canadian Nuclear Safety Commission, Ottawa, Canada

Corresponding author: B. Jeremić, phone (530) 754-9248. fax (530) 754-7872,

email jeremic@ucdavis.edu

1 Abstract

Presented here is an investigation of the seismic response of a massive NPP structures due to full 3D, inclined, un-correlated input motions for different soil and rock profiles. Of particular interest are the effects of soil and rock layering on the response and the changes of input motions (frequency characteristics) due to such layering. In addition to rock/soil layering effects, investigated are also effects of foundation embedment on dynamic response. Significant differences were observed in dynamic response of containment and internal structure founded on surface and on embedded foundations. These differences were observed for both rock and soil profiles. Select results are used to present most interesting findings.

2 Introduction

Seismic response of Nuclear Power Plants (NPPs) has been at the forefront of interest from the very beginning of use of nuclear energy. Significant research has been done over time on the subject seismic response of NPPs (Wolf et al., 1983; Finn et al., 1986; Wagenknecht, 1987; Chang and Belytschko, 1988; Hanada et al., 1988; Wolf, 1989; Halbritter et al., 1998; Elaidi and Eissa, 1998; Venancio-Filho et al., 1997; Ueshima et al., 1997; Saxena and Paul, 2012; Saxena et al., 2011; Wolf, 1989; Ryu et al., 2010).

Seismic response of NPPs is usually quite complex, involving a number of nonlinearities, including:

- Nonlinear response (elastic-plastic, damage, etc.) of soil and rock material adjacent to the foundation,
- Nonlinear response of contact zone between soil/rock and the foundation (gaping, slipping, elastic-plastic, damage),
- Full nonlinear coupling between pore fluid and soil/rock skeleton (which strongly affects the nonlinear response of soil and rock),
- Buoyant effects, where pore fluid pressures on foundations create time varying, nonlinear forces on the foundation (which also strongly affect nonlinear response of the foundation – soil/rock contact zone),
- Nonlinear response of the structure (containment and internal),
- Nonlinear interaction of fluids and structures/solids within the NPP.

In addition to that, seismic wave field features the following complexities:

- Seismic body waves (P and S, which are fully three dimensional (3D), and inclined),
- Seismic surface waves (Rayleigh, Love, etc., which produce three translational and three rotational components of motions at point at and near (at depth) the surface),
- Seismic wave lack of correlations (or incoherence, as it is known in the frequency domain)

Present study focuses on the effects soil/rock layering has on seismic response of an NPP subjected to realistic, 3D, inclined seismic wave field. Moreover, effects of foundation embedment are evaluated as well for two NPP models, one on surface and the other on a 15m embedded foundation.

Paper is organized in two main parts, the first describing the simulation model development, while the second part presents a selected set of results that are used to emphasize main findings.

3 Simulation Model Development

Presented here briefly is the development of the simulation model, including the soil/rock profiles, the finite element model for soil/rock-structure system, input motions development and the simulation platform.

3.1 Soil/Rock Profiles

Soil and rock layering beneath the NPP was assumed to be horizontal. A total of twelve soil (shear wave velocity $V_s \leq 760$m/s) and rock (shear wave velocity $V_s > 760$m/s) models (profiles) were developed. Their spatial distribution and assumed properties (layer thicknesses and shear wave velocities) are presented in Table 1. One of the focuses of the study was to investigated seismic behavior of an NPP founded on a variety of geologic conditions, from hard rock (Case 1) all the way to soil (Case 8), with variations of uniform soil/rock profiles (Cases 1, 2, 4, 6, 8) and layered cases (3, 5, 7, 9, 10, 11, 12). Soil/rock profiles described in Table 1 extend all the way to a depth of 40Km, however Table only gives the top 500m of shear wave velocities (and thus the soil stiffness). Beneath top 500m the soil/rock profiles are marked as either **G** (gradual increase in soil/rock shear wave velocity (stiffness) to values of $V_s = 3200$m/s and above) or as **I** (immediate increase in soil/rock shear wave velocity (stiffness) to a value of $V_s = 4000$m/s.).

It is important to note that profiles 1 and 8 represent the two extremes, while other soil profiles fall in between.

Table 1: Table describing 12 soil profiles used in this study up to a depth of 500m.

	Soil profiles with shear wave velocity [m/s]											
Depth [m]	1	2	3	4	5	6	7	8	9	10	11	12
50	2600	1500	1000	1000	300	300	300	300	300	300	300	300
100											400	2600
150									500	2600	500	
200												
250			1500		2600		750		750		750	
300												
350			2000				1000		1000		1000	
400												
450												
500												
to ∞	**G**	**G**	**G**	**G**	**I**	**I**	**I**	**G**	**I**	**I**	**I**	**I**

3.2 Seismic Motion Modeling

Seismic motions were developed using an analytic solution, developed using Green's functions (Hisada, 1994; Hisada and Bielak, 2003). The method takes into account fault slip mechanism, and propagates the wave through elastic half space layered medium to the surface. The fault rupture mechanics was chosen to be similar to that of Northridge mainshock, which generated an earthquake with a moment magnitude of 6.7. Fault rupture was modeled using Boore's source model, while the seismic waves propagating from that source are modeled using Green's functions for layered half space. As presently implemented, this model can model a minimum period of $T = 0.06$s (corresponding to the frequency of $f = 16.67$Hz). Rupturing fault parameters include: fault length of 18km, fault width of 24km, number of sub-faults along the length and width is 14×14, strike of 122^o, and a dip of 40^o.

Figure 1 shows ground motion model setup. The fault was at the depth of approximately 17km, while the NPP structures (the soil/rock structure model) was placed at approximately 17km away from the earthquake epicenter. The main motivation for a chosen setup was to have a rupturing fault (hypocenter and epicenter) fairly close to the NPP, as was the case of the recent earthquake at the Kashiwazaki NPP in Japan. Moreover, close proximity (in relative terms) of the seismic source will result in the development of significant 3D, inclined, body and surface seismic waves. The actual NPP site, was oriented in such a way to pick up highest horizontal motions in local X direction, as shown in Figure 1.

The Domain Reduction Method. Seismic input is modeled using the Domain Reduction Method Bielak et al. (2003); Yoshimura et al. (2003)). It is a modular, two-step dynamic procedure aimed

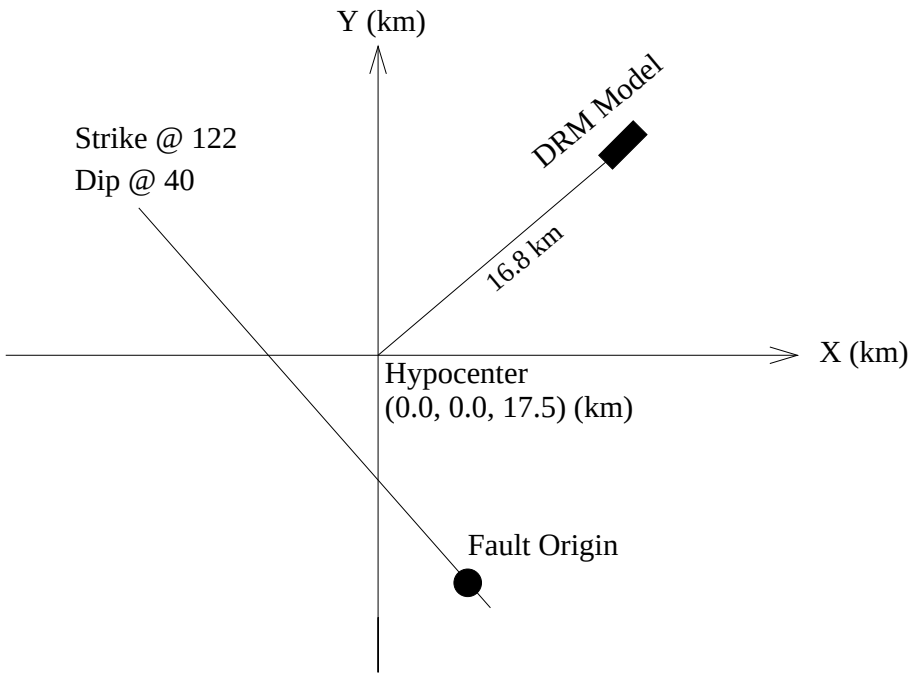

Figure 1: Analytic model (Green's functions) setup, with locations of hypocenter, epicenter and the DRM model.

at reducing the large computational domain to a more manageable size. The DRM replaces forces from the seismic source with dynamically consistent set of forces applied on a single layer of finite element surrounding a soil/rock-structure NPP system. The replacement force, aka an effective force, (P^{eff}) and is given by :

$$P^{eff} = \left\{ \begin{array}{c} P_i^{eff} \\ P_b^{eff} \\ P_e^{eff} \end{array} \right\} = \left\{ \begin{array}{c} 0 \\ -M_{be}^{\Omega+}\ddot{u}_e^0 - K_{be}^{\Omega+}u_e^0 \\ M_{eb}^{\Omega+}\ddot{u}_b^0 + K_{eb}^{\Omega+}u_b^0 \end{array} \right\} \tag{1}$$

Accelerations ($\ddot{u}^0$) and displacements (u^0) are obtained from the free field model (obtained from an analytic solution, described in section 3.2 above) and feature realistic, 3D, inclined seismic waves including both body (P and S) and surface (Rayleigh and Love) waves. Part of the model that is inside a single layer of finite elements where effective forces are applied can be material nonlinear. Additional DRM modeling details are available in Jeremić et al. (2012).

3.2.1 Lack of Correlation (Incoherence) for the Original Seismic Motions

Figure 2 shows the analysis of analytically developed seismic motions (using Green's functions for layered half space) with incoherence function developed from the Lotung LSST site in Taiwan by Abrahamson et al. (1991); Abrahamson (1992a, 2005, 1992b). For each of the twelve simulations the x-components of points 1 and 2, were used to estimate lagged coherency. To be consistent with

the incoherence function, the lagged coherency is calculated on the strong motion window using an 11-point Hamming window. Lagged coherency between the pairs of the synthetic motions is

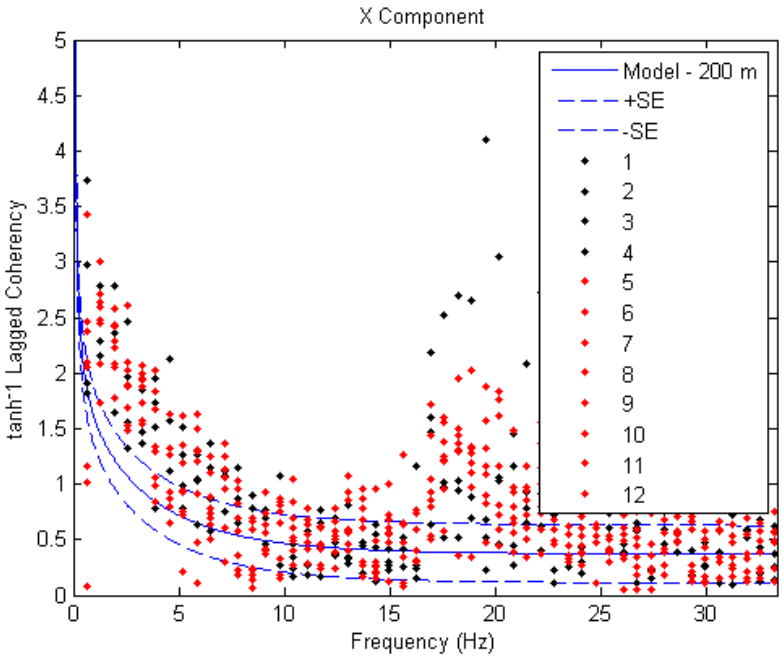

Figure 2: A comparison incoherence of analytically developed seismic motions (using Green's functions for layered half-space) with incoherence model by Abrahamson, from Lotung LSST site, for all twelve soil/rock profiles, grouped as rock (1-4, black markers) and soil (5-12, red markers) profiles.

biased higher (i.e. more coherent) at frequencies up to approximately 7Hz as shown in Figure 2. The large spike in lagged coherency at 16 Hz is due to a 16 Hz frequency limit of the synthetic motions developed using layered half space model.

It is interesting to note that even a model with quite regular layering, simulated over half space, is able to predict incoherence, although to a smaller degree than what the extrapolated model from Lotung LSST site shows. These results signify that a dimension of the model (in this case half-space) plays an important role in development of the incoherence, since it was shown by Walling (2009), that a limited size model (a block with sides of 1km) cannot account for a majority of incoherence.

3.2.2 Lack of Correlation (Incoherence) for the Abrahamson Model Motions

In addition to (partially) incoherent motions developed using layered half space simulations, an additional (different) set of incoherent motions was developed in order to test the effects inco-

herency has on NPP response. In order to introduce appropriate amount of variability over the bandwidth due to incoherence effects, each point was used as a seed motion to generate a new motion across the grid at a separation distance of 200 meters. In other words point 1 is modified to generate a ground motion at point 2 and vice versa. The method of introducing incoherence effects is called Frequency Dependent Windowing (FDW) (Ancheta et al., 2012). The method is a non-stationary simulation routine that utilizes a modified short-time Fourier transform (MSTF) routine for which spectral modifications are made consistent with a selected coherency model. The MSTF routine allows preservation of the non-stationary properties of the motion and incorporation of time-varying non-linear spectral modifications. The routine is summarized below:

1. The seed time series is split into short time segments.
2. A discrete Fourier transform (DFT) is applied to the segments.
3. Fourier amplitudes and phase angles at each frequency within a desired frequency range (dependent on segment length) are modified consistent to a coherency function for each segment (Ancheta, 2010).
4. The new set of Fourier phase angles is combined with the new set of Fourier amplitudes and transformed into the time domain with an inverse Fourier transform (IFT).
5. The modified short time segments are recombined to form a modified time series.
6. Steps 1-5 are performed multiple times for multiple segment lengths, with each segment length having a specified frequency range over which phase angles are modified. Hence, multiple modified time series are created. Segment lengths and corresponding frequency limits used are shown in Table 2.
7. The multiple modified time series are match-filtered (i.e., band-pass filtered with the limits of the pass-band matching the band of the modification) to combine the modified frequency bands in the frequency domain.
8. The non-overlapping frequency bands are inverted with an IFT to create the final broadband modified time series.

Description of Selected Incoherence Models. Synthetic models created by analytic solution for layered half space, with different profiles but similar source were used as seed motions for incoherence motion development. Soil/Rock profiles as described in Table 1 were used and grouped as rock cases (1-4) with $V_s \geq 760$m/s and soil cases (5-12) with $V_s < 760$m/s.

Table 2: Segment duration (L) and frequency bands (b) used in the FDW routine. T is the duration of the seed series.

Segment duration, L_i [sec]	Frequency limits , b_i [Hz]
1.28	2-Nyquist
2.56	1-2
5.12	0.5-1
10.24	0.25-0.5
20.48	0.12-0.25
T	0-0.12

Separate coherency and random Fourier amplitude models are selected for rock (1-4) and soil (5-12) profiles separately. For soil cases 1-4, a plane wave coherency (γ_{pw}) and $\sigma_{\Delta A}$ developed by Abrahamson (2007) from the Pinyon Flat array recordings located in California was selected. These models are shown in equations 2 and 3 and Table 3

$$\gamma_{pw}(f,\xi) = \left[1 + \left(\frac{f\tanh(a_3\xi)}{a_1 f_c(\xi)}\right)^{n1(\xi)}\right]^{-1/2}\left[1 + \left(\frac{f\tanh(a_3\xi)}{a_2}\right)^{n2}\right]^{-1/2} \tag{2}$$

$$\sigma_{\Delta A}(f,\xi) = 0.79(1 - e^{-0.45-0.0017\xi)f}) \tag{3}$$

Table 3: Plane-wave coherency model coefficients for the horizontal component.

Coefficient name	Horizontal coefficient value
a_1	1.0
a_2	40
a_3	0.4
$n_1(\xi)$	$3.80 - 0.040\ln(\xi+1) + 0.0105\left[\ln(\xi+1) - 3.6\right]^2$
n_2	16.4
$f_c(\xi)$	$27.9 - 4.82\ln(\xi+1) + 1.24\left[\ln(\xi+1) - 3.6\right]^2$

For soil cases (5-12), a lagged coherency ($|\gamma|$) and $\sigma_{\Delta A}$ developed by Ancheta (2010) from the Lotung LSST (Large Scale Seismic Test) and BVDA (Borrego Valley Differential Array) recordings located in Taiwan and California, respectively, was selected. The models are shown in equations 4 and 5.

$$\tanh^{-1}|\gamma(f,\xi)| = (3.79 - 0.499(\ln\xi))\exp\left((-0.115 - 0.0084\xi)f\right) + \frac{1}{3}(\xi)f^{-0.878(\xi)} + 0.35 \tag{4}$$

$$\sigma_{\Delta A}(f,\xi) = (1 - e^{-0.1005 - 0.0025\xi)f})$$

(5)

Plane wave coherency is typically lower than lagged coherency as it includes random variations in the wave passage effect. The plane wave coherency model was selected instead of a lagged coherency model as there are no available lagged coherency models available for rock sites comparable to eastern North America rock sites.

Range of Incoherence Model Applicability Based on a report by Abrahamson (2007) the incoherence models developed from the Pinyon Flat array appears to be applicable to separation distances of 5 to 150 meters and a frequency range of from 5 to 40 Hz. Since the model is developed from Pinyon Flat recordings alone. it is unknown how well this model fits similar rock site array recordings or possible future array recordings located in the eastern North America region.

The incoherence models developed by Ancheta (2010) are a slight modification of incoherence models developed by Abrahamson (1992a) and are applicable to separation distances of 6 to 160 meters and frequencies greater than 1 Hz.

Both models have been extrapolated to 200 meters for the process of including incoherence using the FDW routine. In a comparison of coherency from the SMART 1 and LSST array in Taiwan, Abrahamson (1992a) concluded that the decay in coherency was similar up to 200m.

3.3 Finite Element Model

Full 3D finite element models were developed for both surface foundation and embedded foundation NPPs. Structural models (containment and internal structures) consisted of modal equivalent stick model.

Containment Structure Modal Equivalent Stick Model was modeled using twelve (12) 3D elastic beam elements, where each stick has its properties calculated from the cylindrical and/or half sphere part of the containment structure. Three moments of inertia were used (two bending and one torsional), while lumped masses included both translational and mass moments of inertia.

Internal Structure Modal Equivalent Stick Model consists of sixteen nodes, connected with elastic beam elements as well as rigid connections (where center of mass is not on the beam axes). Stiffness properties were characterized with bending moments of inertia (two in 3D), coordinates of stiffness center, moment of inertia in torsion and shear area. Since for the internal structure, centers of mass do not coincide with centers of the stiffness, rigid connection elements were used to place lumped mass elements away from stiffness centers.

Foundation Slab was placed at the bottom of both containment and internal structures (connection at the same node). Since foundation slab was modeled using brick (solid) elements, a rectangular/cross beam structure was placed on top of the foundation slab to provide for stability of above beam models (containment and internal stick models). In addition to providing for the stability of containment and internal stick models, this rectangular/cross beam structure also provided additional stiffness for the foundation slab that was missing since containment structure (in reality a thick shell with certain horizontal spatial extent) is replaced with a stick model. Addition of rectangular/cross beam structure was done for both surface and embedded foundation models. The foundation slab has dimensions of 100m $\times$ 150m and a thickness of 3.5m. For the surface foundation, the lower level of concrete is at the depth of 5m while for the embedded it is at the depth of 15m.

The 3D finite element models for a soil/rock block have dimensions of 200m (lenght) $\times$ 140m (width) $\times$ 60m (depth). They consist of eight node brick elements with linear interpolation of displacements and dimensions of 5m $\times$ 5m $\times$ 5m. With chosen dimension of the finite element, different types of soil/rock material models (stiffness) will be able to accurately model different frequencies of motions:

- Rock with shear wave velocity of $v_s = 2600$m/s, and with the element size of $h = 5$m is able to model (with small error, below 10%) frequencies of up to $f_{max} = 65$Hz, while any frequencies above that will be modeled with increased error,
- Similar to the above case for rock with shear wave velocity of $v_s = 1500$m/s, and element dimension of $h = 5$m, accurate modeling of frequency of $f_{max} = 37$Hz is expected, while anything above that will introduce larger error,
- Rock with $v_s = 1000$m/s, and element size $h = 5$m, will accurate model $f_{max} = 25$Hz;
- While soil with shear wave velocity of $v_s = 300$m/s, and element size of $h = 5$m, will accurately model $f_{max} = 7$Hz, while for higher frequencies, the error will be larger.

For all the finite element models, Newmark numerical time stepping algorithm was used (Newmark (1959)), with time step increment of $\delta t = 0.015$s. A small amount of numerical damping was introduced through Newmark algorithms constants $\gamma = 0.6000$ $\beta = 0.3025$ in order to damp out high frequencies that are present due to the finite element discretization process Hughes (1987), Argyris and Mlejnek (1991).

Figures 3 and 4 show a 3D finite element model for a case of surface and embedded foundation, respectively. In addition to the modal equivalent stick models for a containment and internal structures, model includes a concrete slab, the DRM layer, the soil/rock inside the DRM layer and the material outside the DRM layer.

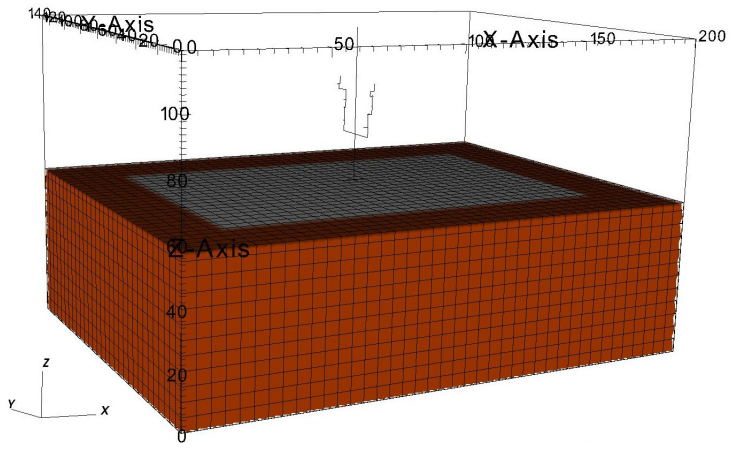

Figure 3: Surface foundation model with underlying rock/soil and the equivalent elastic stiffness and mass superstructure model representing NPP.

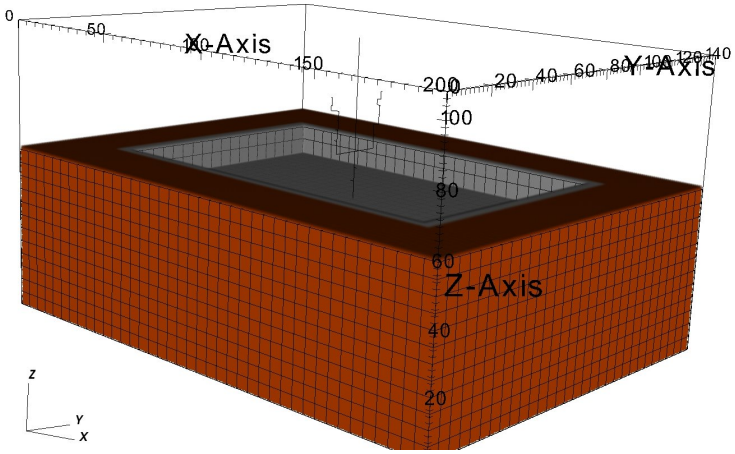

Figure 4: Embedded foundation model with underlying rock/soil and the equivalent elastic stiffness and mass superstructure model representing NPP.

3.4 Simulation Platform

Finite element program used in this study was developed using a number of numerical libraries, algorithms, material models and finite elements available through one of open source licenses. The finite element domain was managed using Modified OpenSees Services (MOSS) library (Jeremić et al., 1989-2012; Jeremić and Jie, 2007, 2008; McKenna, 1997). On a lower functional level, a set of NewTemplate3Dep numerical libraries (Jeremić and Yang, 2002) was used for constitutive level modeling, while nDarray numerical libraries (Jeremić and Sture, 1998) are used to handle vector, matrix and tensor manipulations, and element libraries from UCD CompGeoMech

FEMtools (Jeremić et al., 1989-2012) are used to supply other necessary libraries and components. The solution of system of equations was provided by UMFPACK solver (Davis and Duff, 1997b,a, 1999; Davis, 2004a,b).

Numerical simulation system used in this study is a precursor to the NRC ESSI Simulator modeling and simulation system that is currently undergoing a very active development (expansion, documentation, verification and validation, etc.) (Jeremić et al., 2011).

4 Select Results

A large number of test cases were analyzed and a wealth of results developed. Presented here is a select number of results that are used to emphasize main findings related to the influence of variable layered soil/rock under the surface and embedded foundation slab.

4.1 Comparison of Responses Between NPP Structures on a Variable Stiffness Single Layer Base Soil/Rock

Presented here are results for behavior of the NPP on surface and embedded foundation with variable thickness of a uniform soil/rock layer. In particular, four rock/soil profiles (all with uniform rock/soil up to the depth of 500m) are used to emphasize differences. The following profiles are used:

- Case 1 ($v_s = 2600$m/s to a depth of 500m),
- Case 2 ($v_s = 1500$m/s to a depth of 500m),
- Case 4 ($v_s = 1000$m/s to a depth of 500m),
- Case 8 ($v_s = 300$m/s to a depth of 500m)

where a more detailed description of profiles is given in Table 1.

Results of four different uniform profiles (from hard rock, to soil, Cases 1, 2, 4 and 8) are used to show that softer foundation soil/rock does filter out higher frequencies as well as de-amplify motions for higher frequencies at the top of both containment and internal structures. Behavior is quite the opposite at lower frequencies, where softer soil/rock amplify motions and contributes to (in some cases) significant amplification of motions (particularly for frequencies below 1Hz).

Figures 5 and 6 show response for surface and embedded foundation models, respectively.

There are a number of observations that can be made:

- There is a slight increase in base motions for all four cases for surface foundation (when compared to embedded foundations) for lower frequencies, below 4Hz, while there is a

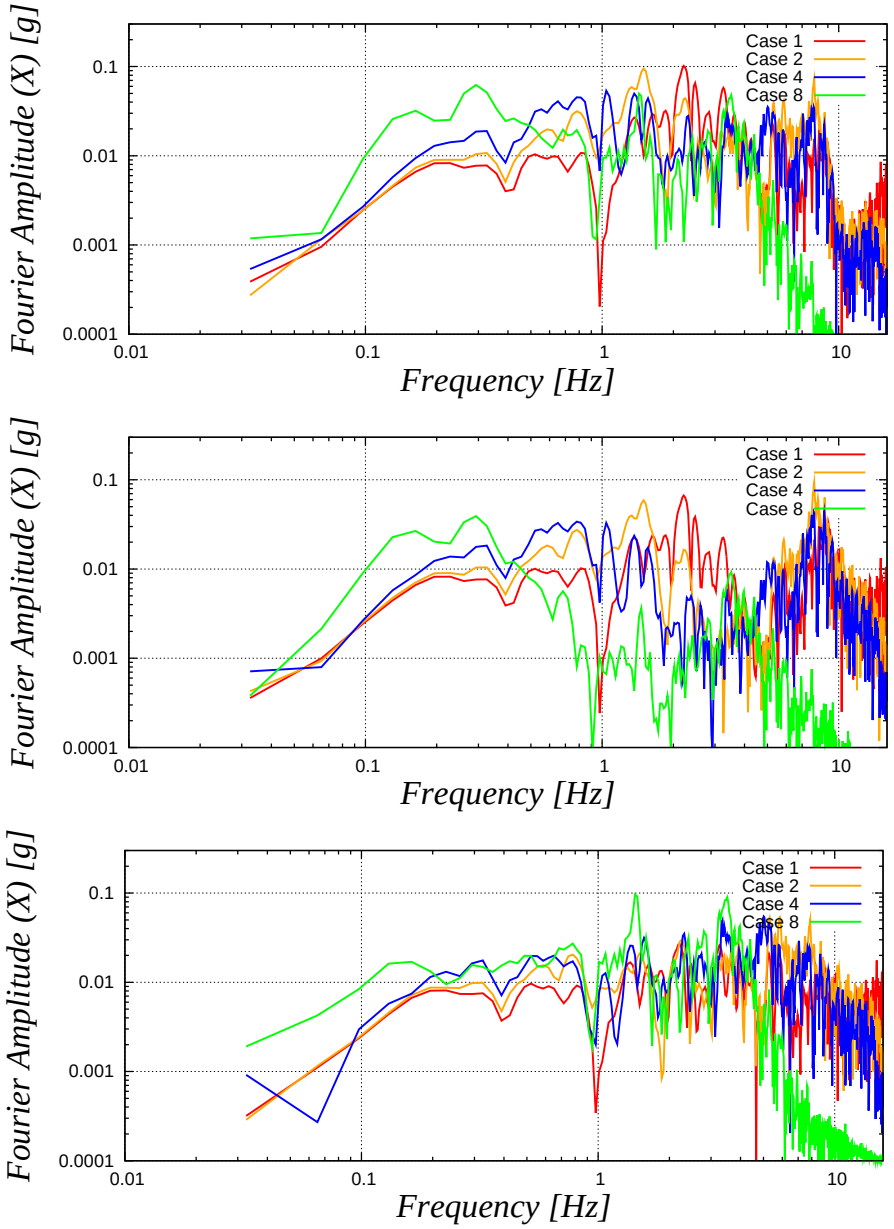

Figure 5: Comparison of acceleration FFTs for cases 1, 2, 4, 8 for horizontal direction at the (upper) **top of containment structure**, (middle) **top of internal structure**, and (bottom) **the base of containment and internal structures** on a **surface foundation**.

larger decrease (for surface foundations when compared to embedded foundations) for frequencies above 4Hz for all cases, with particularly large decrease for soil (Case 8) (compare bottom in Figures 5 and 6).

- For structural response on embedded foundation (compare middle and upper in figures 5) and Figures 6) the internal and containment structure react quite differently at frequencies

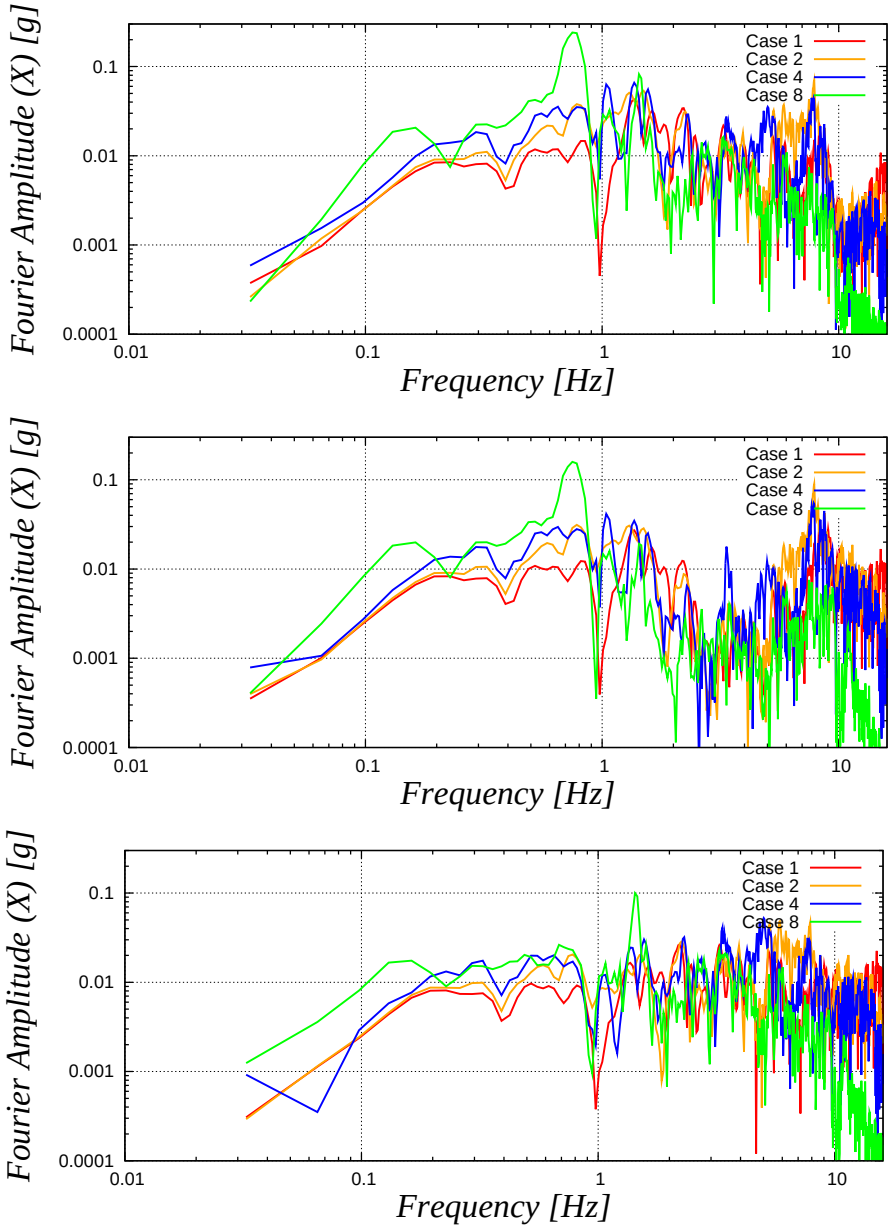

Figure 6: Comparison of acceleration FFTs for cases 1, 2, 4, 8 in horizontal direction at the (upper) **top of containment structure**, (middle) **top of internal structure**, (bottom) **base of internal and containment structures** on an **embedded foundation**.

above 2Hz, for different soil/rock stiffness beneath the foundation. It is particularly important to note that the embedded foundation seems to reduce motions of both containment and internal structures for frequency range of 1Hz to 5Hz (significantly) while motions remain almost the same for a frequency range above 5Hz. This can be explained by the fact that for the embedded foundation, the energy of surface waves (Rayleigh waves in this case) is much smaller for embedded foundation and with that, the rotational components of motions

are not exciting structure (containment and internal) as much as for the surface foundation case. This conclusion, however cannot be drawn in general as there might be cases where the lack of surface waves (at depth) might not be beneficial to the dynamic response.

- The soil subsurface condition (Case 8) does consistently show the lower response for higher frequencies, and higher response for lower frequencies, This is, of course to be expected, and will only be amplified if real soil/rock non-linearities are taken into account (only linear elastic material properties were used in this study).

- Response of the structures on surface foundations is fairly similar for containment structure with significant divergence of response only after about 4Hz (again the soil case does diverge the most). On the other hand, the internal structure has a very different response on different soil/rock layers. Soil profile shows again the most divergence for both containment and internal structure reduction in response only for frequencies higher than 6Hz.

4.2 Comparison of Responses Between NPP Structures on Variable Thickness Soft Soil Layer

In addition to the above uniform profiles, analyzed were profiles with a varying thickness of a soil layer ($v_s = 300$m/s) (cases 6, 5, 10 and 12) where the thickness was varying:

- Case 6, top 500m of soil with $v_s = 300$m/s, below that is a hard rock ($v_s = 2600$m/s),

- Case 5, top 200m of soil with $v_s = 300$m/s, below that is a hard rock ($v_s = 2600$m/s),

- Case 10, top 100m of soil with $v_s = 300$m/s, below that is a hard rock ($v_s = 2600$m/s),

- Case 12, top 50m of soil with $v_s = 300$m/s, below that is a hard rock ($v_s = 2600$m/s).

Figure 7, shows seismic response at the top and base of containment and internal structures for the surface foundation, while Figure 8 show response of the top and base of containment and internal structures on embedded foundation.

A number of observation can be made:

- A significant differences are observed in responses between surface and embedded foundation structures (both for containment and internal structures).

- For example, internal structure (middle figures in Figures 7 and 8) show significant differences, and in general the embedded foundation internal structure has amplified motions when compared with the surface foundation case.

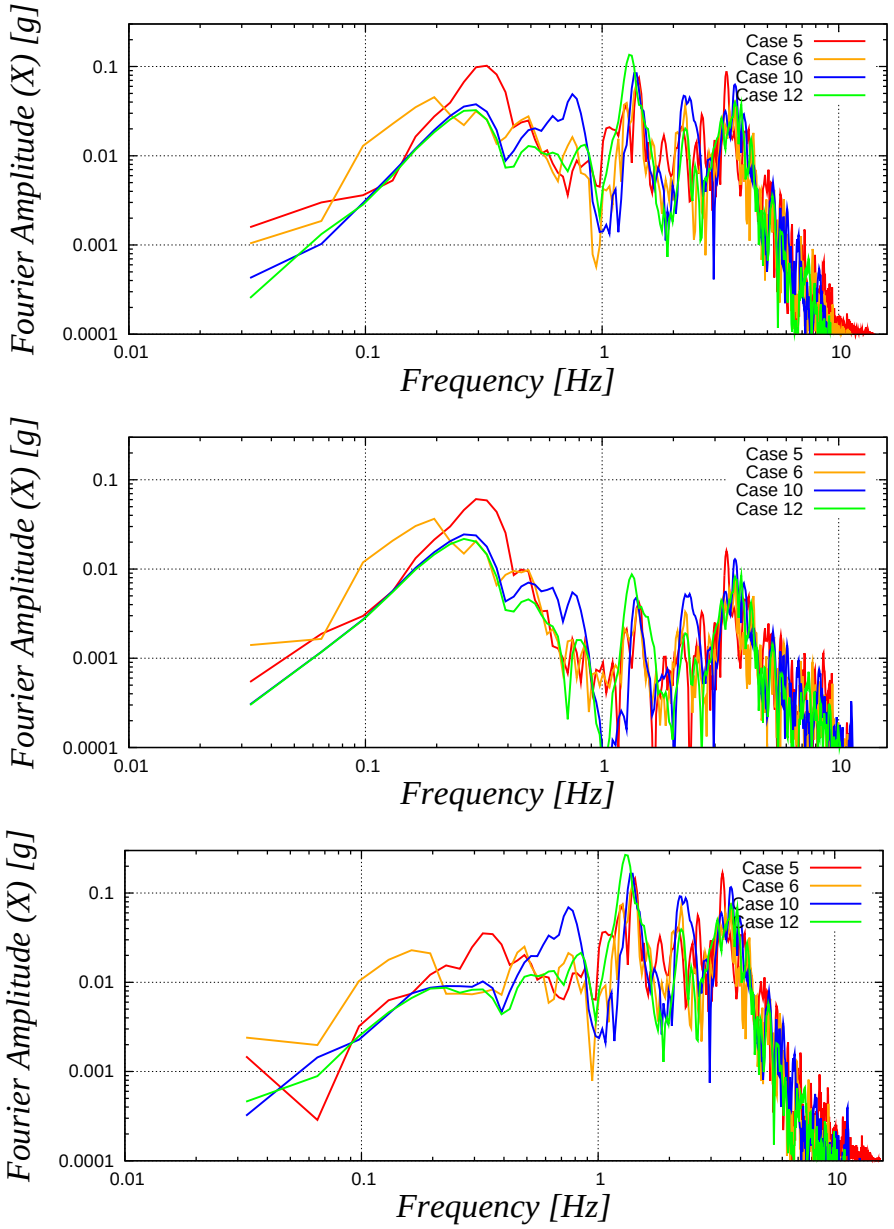

Figure 7: Comparison of acceleration FFTs for cases 5, 6, 10, 12 for horizontal direction at the (upper) **top of a containment structure**, (middle) **top of an internal structure**, and (bottom) **base of containment and internal structures** on a **surface foundation**.

- On the other hand, containment structure (upper figures in Figures 7 and 8) show amplification for embedded foundation case only below about 1.5Hz and above 4Hz, while in the range $1.5 - 4$Hz, the surface foundation has larger amplifications.

- The thickness of the soft soil layer (it varies from 50m to 500m) does not affect much the response of either containment or internal structures at higher frequencies. Presented

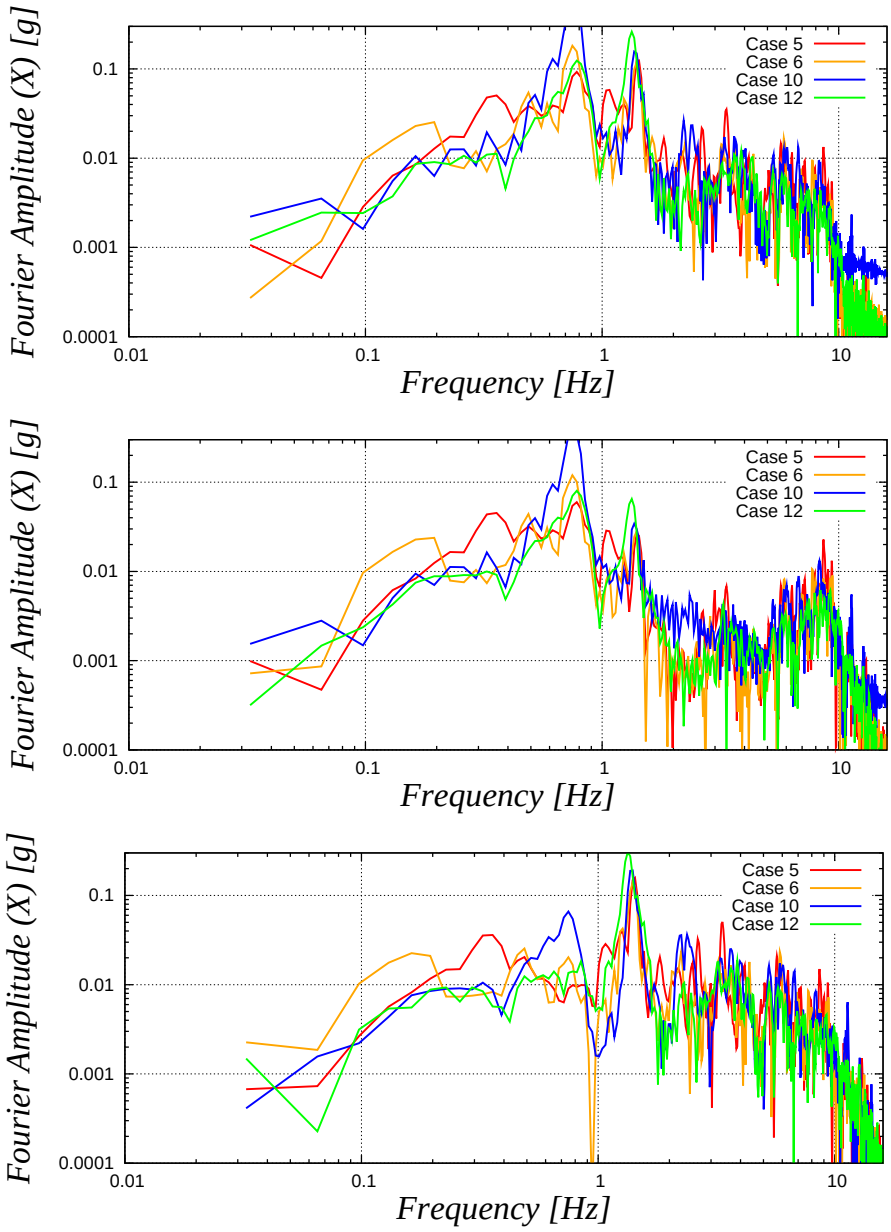

Figure 8: Comparison of acceleration FFTs for cases 5, 6, 10, 12 for horizontal direction at the (upper) **top of a containment structure**, (middle) **top of a internal structure**, and (bottom) **base of containment and internal structures** on an **embedded foundation**.

Fourier Amplitudes suggest that a small variation of response is to be expected for variable thickness of soft soil layer, particularly for frequencies above approximately 2Hz. Below such frequency, response does differ, in some cases more significant that in other. This behavior is somewhat expected, as the soft soil layer "isolates" the structures from higher frequencies, while the lower frequencies do get certain amplification, depending on the layer thickness, stiffness and mass. This is most obvious for the frequencies of about 0.8Hz where the amplification factors seems to differ by an order of magnitude between various cases.

- Independent of the soft soil layer thickness, significant reduction of higher frequencies is noticeable, which is apparent in Figure 8.

5 Summary

Presented in this paper was an investigation of the seismic response of a massive NPP soil/rock-structure system (both containment and internal structures, with the foundation slab (surface and/or embedded) and with a significant soil/rock volume) due to full 3D, inclined, un-corellated body and surface seismic motions for a different soil/rock profiles. Presented was an investigation of the importance of soil/rock layering on response of containment and internal structures to realistic seismic motions. In addition to that, an investigation of effects of foundation embedment was also performed for all soil/rock layering cases.

A number of specific conclusions can be made for each of the soil/rock layer cases, and such conclusions were made in the above results section. It is, however, very important to note that presented results do suggest that each soil/rock layering system features behavior specific for that particular layering, for particular structural system (containment and/or internal) and for a particular (realistic) earthquake motion, landing to the conclusion that the interaction of all three components, the earthquake, the soil/rock and the structure play crucial role in dynamic response of an NPP.

6 Acknowledgment

Work presented here was funded by a grant from the Canadian Nuclear Safety Commission (SNSC) and such support is greatly appreciated.

References

N. Abrahamson. Spatial variation of earthquake ground motion for application to soil-structure interaction. *EPRI Report No. TR-100463, March.*, 1992a.

N. Abrahamson. Generation of spatially incoherent strong motion time histories. In A. Bernal, editor, *Earthquake Engineering, Tenth World Conference*, pages 845–850. Balkema, Rotterdam, 1992b. ISBN 90 5410 060 5.

N. Abrahamson. Updated coherency model. *Report Prepared for Bechtel Corporation, April*, 2005.

N. A. Abrahamson. Hard rock coherency functions based on Pinyon Flat data. unpublished data report, 2007.

N. A. Abrahamson, J. F. Schneider, and J. C. Stepp. Empirical spatial coherency functions for applications to soil–structure interaction analysis. *Earthquake Spectra*, 7(1):1–27, 1991.

T. Ancheta, J. Stewart, and N. Abrahamson. Frequency dependent windowing: A non-stationary method for simulating spatially variable earthquake ground motions. *Earthquake Spectra*, 2012. in review.

T. D. Ancheta. *Engineering characterization of spatially variable earthquake ground motions*. PhD thesis, University of California at Los Angeles, 2010.

J. Argyris and H.-P. Mlejnek. *Dynamics of Structures*. North Holland in USA Elsevier, 1991.

J. Bielak, K. Loukakis, Y. Hisada, and C. Yoshimura. Domain reduction method for three–dimensional earthquake modeling in localized regions. part I: Theory. *Bulletin of the Seismological Society of America*, 93(2):817–824, 2003.

H. S. Chang and T. Belytschko. Multi-scattering and boundary effects in soil-structure interaction. *Nuclear Engineering and Design*, 106(1):9 – 17, 1988. ISSN 0029-5493. doi: 10.1016/0029-5493(88)90266-X. URL `http://www.sciencedirect.com/science/article/pii/002954938890266X`.

T. Davis. A column pre-ordering strategy for the unsymmetric-pattern multifrontal method. *ACM Transactions on Mathematical Software*, 30(2):165–195, 2004a. URL `http://doi.acm.org/10.1145/992200.992205`.

T. Davis. Algorithm 832: Umfpack, an unsymmetric-pattern multifrontal method. *ACM Transactions on Mathematical Software*, 30(2):196–199, 2004b. URL `http://doi.acm.org/10.1145/992200.992206`.

T. Davis and I. Duff. A combined unifrontal/multifrontal method for unsymmetric sparse matrices. *ACM Transactions on Mathematical Software*, 25(1):1–19, 1999. URL http://doi.acm.org/10.1145/305658.287640.

T. A. Davis and I. S. Duff. An unsymmetric–pattern mutlifrontal method for sparse LU factorization. *SIAM Journal of Matrix Analysis and Applications*, 18(1):140–158, 1997a.

T. A. Davis and I. S. Duff. A combined unifrontal/multifrontal method for unsymmetric sparse matrices. Technical Report TR97-016 (UofF) and TR-97-046 (RAL), University of Florida and Rutherford Appleton Laboratory, 1997b.

B. M. Elaidi and M. A. Eissa. Soil-structure interaction in fuel handling building. *Nuclear Engineering and Design*, 181(1-3):145 – 156, 1998. ISSN 0029-5493. doi: 10.1016/S0029-5493(97)00341-5. URL http://www.sciencedirect.com/science/article/pii/S0029549397003415.

W. Finn, R. Ledbetter, and L. Beratan. Seismic soil-structure interaction: Analysis and centrifuge model studies. *Nuclear Engineering and Design*, 94(1):53 – 66, 1986. ISSN 0029-5493. doi: 10.1016/0029-5493(86)90153-6. URL http://www.sciencedirect.com/science/article/pii/0029549386901536.

A. Halbritter, N. Krutzik, Z. Boyadjiev, and T. Katona. Dynamic analysis of vver type nuclear power plants using different procedures for consideration of soil-structure interaction effects. *Nuclear Engineering and Design*, 182(1):73 – 92, 1998. ISSN 0029-5493. doi: 10.1016/S0029-5493(97)00292-6. URL http://www.sciencedirect.com/science/article/pii/S0029549397002926.

K. Hanada, T. Iwatate, Y. Sawada, and H. Ezure. Soil-structure interaction of "jpdr" based on earthquake observations and forced vibration tests. *Nuclear Engineering and Design*, 105(2):173 – 183, 1988. ISSN 0029-5493. doi: 10.1016/0029-5493(88)90338-X. URL http://www.sciencedirect.com/science/article/pii/002954938890338X.

Y. Hisada. An efficient method for computing Green's functions for a layered half-space with sources and receivers at close depths. *Bulletin of the Seismological Society of America*, 84(5):1456–1472, 1994.

Y. Hisada and J. Bielak. A theoretical method for computing near–fault ground motions in layered half–spaces considering static offset due to surface faulting, with a physical interpretation of fling step and rupture directivity. *Bulletin of the Seismological Society of America*, 93(3):1154–1168, 2003.

T. Hughes. *The Finite Element Method ; Linear Static and Dynamic Finite Element Analysis*. Prentice Hall Inc., 1987.

B. Jeremić and G. Jie. Plastic domain decomposition method for parallel elastic–plastic finite element computations in gomechanics. Technical Report UCD–CompGeoMech–03–07, University of California, Davis, 2007. available online: `http://sokocalo.engr.ucdavis.edu/~jeremic/wwwpublications/CV-R24.pdf`.

B. Jeremić and G. Jie. Parallel soil–foundation–structure computations. In N. L. M. Papadrakakis, D.C. Charmpis and Y. Tsompanakis, editors, *Progress in Computational Dynamics and Earthquake Engineering*. Taylor and Francis Publishers, 2008.

B. Jeremić and S. Sture. Tensor data objects in finite element programming. *International Journal for Numerical Methods in Engineering*, 41:113–126, 1998.

B. Jeremić and Z. Yang. Template elastic–plastic computations in geomechanics. *International Journal for Numerical and Analytical Methods in Geomechanics*, 26(14):1407–1427, 2002.

B. Jeremić, Z. Yang, Z. Cheng, G. Jie, K. Sett, M. Taiebat, M. Preisig, N. Tafazzoli, P. Tasiopoulou, J. A. A. Mena, and F. Pisanò. Lecture notes on computational geomechanics: Inelastic finite elements for pressure sensitive materials. Technical Report UCD-CompGeoMech–01–2004, University of California, Davis, 1989-2012. available online at: `http://sokocalo.engr.ucdavis.edu/~jeremic`.

B. Jeremić, A. Kammerer, N. Tafazzoli, and B. Kamrani. The NRC ESSI Simulator. In B.K.Dutta, editor, *Proceedings of the 21st SMiRT (Structural Mechanics in Reactor Technology) Conference*, 2011. Paper # 550.

B. Jeremić, N. Tafazzoli, B. Kamranimoghaddam, C.-G. Jeong, J. A. A. Mena, and F. Pisanò. The NRC ESSI Notes (DRAFT). Technical report, University of California, Davis CA, and Lawrence Livermore National Laboratory, Berkeley, CA, 2012. Draft available online at: `http://nrc-essi-simulator.info`.

F. T. McKenna. *Object Oriented Finite Element Programming: Framework for Analysis, Algorithms and Parallel Computing*. PhD thesis, University of California, Berkeley, 1997.

N. M. Newmark. A method of computation for structural dynamics. *ASCE Journal of the Engineering Mechanics Division*, 85:67–94, July 1959.

J.-S. Ryu, C.-G. Seo, J.-M. Kim, and C.-B. Yun. Seismic response analysis of soil-structure interactive system using a coupled three-dimensional fe-ie method. *Nuclear Engineering and*

Design, 240(8):1949 – 1966, 2010. ISSN 0029-5493. doi: 10.1016/j.nucengdes.2010.03.028. URL http://www.sciencedirect.com/science/article/pii/S0029549310002062.

N. Saxena and D. Paul. Effects of embedment including slip and separation on seismic ssi response of a nuclear reactor building. *Nuclear Engineering and Design*, 247(0):23 – 33, 2012. ISSN 0029-5493. doi: 10.1016/j.nucengdes.2012.02.010. URL http://www.sciencedirect.com/science/article/pii/S002954931200088X.

N. Saxena, D. Paul, and R. Kumar. Effects of slip and separation on seismic ssi response of nuclear reactor building. *Nuclear Engineering and Design*, 241(1):12 – 17, 2011. ISSN 0029-5493. doi: 10.1016/j.nucengdes.2010.10.011. URL http://www.sciencedirect.com/science/article/pii/S0029549310006904.

T. Ueshima, T. Kokusho, T. Okamoto, and H. Yajima. Seismic response analysis of embedded structure at hualien, taiwan. *Nuclear Engineering and Design*, 172(3):289 – 295, 1997. ISSN 0029-5493. doi: 10.1016/S0029-5493(97)00052-6. URL http://www.sciencedirect.com/science/article/pii/S0029549397000526.

F. Venancio-Filho, F. de Barros, M. Almeida, and W. Ferreira. Soil-structure interaction analysis of npp containments: substructure and frequency domain methods. *Nuclear Engineering and Design*, 174(2):165 – 176, 1997. ISSN 0029-5493. doi: 10.1016/S0029-5493(97)00076-9. URL http://www.sciencedirect.com/science/article/pii/S0029549397000769.

E. Wagenknecht. Response of a npp reactor building under seismic action with regard to different soil properties. *Nuclear Engineering and Design*, 104(2):187 – 195, 1987. ISSN 0029-5493. doi: 10.1016/0029-5493(87)90298-6. URL http://www.sciencedirect.com/science/article/pii/0029549387902986.

M. A. Walling. *Non-Ergodic Probabilistic Seismic Hazard Analysis and Spatial Simulation of Variation in Ground Motion*. PhD thesis, University of California at Berkeley, Spring 2009. Under guidance of Professor Norman Abrahamson.

J. P. Wolf. Soil-structure-interaction analysis in time domain. *Nuclear Engineering and Design*, 111(3):381 – 393, 1989. ISSN 0029-5493. doi: 10.1016/0029-5493(89)90249-5. URL http://www.sciencedirect.com/science/article/pii/0029549389902495.

J. P. Wolf, P. Obernhuber, and B. Weber. Response of a nuclear power plant on aseismic bearings to horizontally propagating waves. *Earthquake Engineering & Structural Dynamics*, 11(4):483–499, 1983. ISSN 1096-9845. doi: 10.1002/eqe.4290110404. URL http://dx.doi.org/10.1002/eqe.4290110404.

C. Yoshimura, J. Bielak, and Y. Hisada. Domain reduction method for three–dimensional earthquake modeling in localized regions. part II: Verification and examples. *Bulletin of the Seismological Society of America*, 93(2):825–840, 2003.